INSTITUT DE FRANCE
Académie des sciences

Comptes Rendus
Mécanique

Yifei Sun and Jiancheng Zhang

Fractional stress-dilatancy equation based on critical state lines with arbitrary form

Volume 349, issue 1 (2021), p. 167-178

Published online: 17 March 2021

https://doi.org/10.5802/crmeca.78

Les Comptes Rendus. Mécanique *sont membres du Centre Mersenne pour l'édition scientifique ouverte*
www.centre-mersenne.org
e-ISSN : 1873-7234

Comptes Rendus
Mécanique
2021, 349, nº 1, p. 167-178
https://doi.org/10.5802/crmeca.78

Short paper / *Note*

Fractional stress-dilatancy equation based on critical state lines with arbitrary form

Yifei Sun *, [a, b] **and Jiancheng Zhang** [c]

[a] Key Laboratory of Ministry of Education for Geomechanics and Embankment Engineering, Hohai University, China

[b] Faculty of Civil and Environmental Engineering, Ruhr Universität Bochum, 44780 Bochum, Germany
URL: http://www6.rz.rub.de:9103/lehrstuhl/team/sun.html.de

[c] School of Naval Architecture and Civil Engineering, Jiangsu University of Science and Technology, Zhangjiagang 215600, Jiangsu, China

E-mails: yifei.sun@rub.de (Y. Sun), zjc5108@just.edu.cn (J. Zhang)

Abstract. The original state-dependent fractional stress-dilatancy (FSD) equation for soils is developed based on the critical state lines (CSLs) with linear form. However, experimental evidences showed that the CSLs of soil in the p'–q and e–p' planes could be both nonlinear as well due to significant material degradation. This note aims to propose a unified FSD equation for soils with arbitrary types of CSLs. Detailed derivations are provided. To validate the proposed FSD equation, a series of triaxial test results of ballast and rockfill are simulated.

Keywords. Fractional derivative, Fractional plasticity, Stress-dilatancy, Sand, Rockfill, State dependence.

Manuscript received 8th December 2019, revised 29th June 2020, accepted 17th February 2021.

1. Introduction

The plastic flow of soil, for example, sand [1–4] and clay [5, 6], were often reported to be state-dependent and nonassociated. To capture such behaviour, Been and Jefferies [3] first introduced the concept of state dependence into critical state soil mechanics (CSSM), by evaluating a series of triaxial test results of different sands. Soon, this concept was widely accepted by many researchers for constitutive modelling of different geomaterials [7, 8]. It can be found that in classic critical-state approaches, characterisation of the state-dependent behaviour usually relied on the incorporation of an additional plastic potential and an empirical state parameter. Even though good model performances were often observed, the basic mathematical principles underlying

* Corresponding author.

the state-dependent stress-dilatancy phenomenon was more or less unclear. Unlike classic approaches, the state-dependent nonassociated behaviour of soil can be simultaneously characterised through the yielding surface in fractional plasticity [9, 10]. By conducting fractional differentiation of a yielding surface, the state-dependent stress-dilatancy (or plastic flow) phenomenon reported by Been and Jefferies [3] was analytically captured, where the state dependence was modelled via the stress distance from the current state to the corresponding critical state of soil. Nevertheless, the developed state-dependent fractional stress-dilatancy (FSD) equation was based on the assumption of a linear critical state line (CSL), which may not be suitable for modelling soils with nonlinear CSLs. Actually, due to the specific physical properties of soil aggregates, curved CSLs with various directional bending in the p'–q and e–p' planes could be also observed in crushable soils [11–13] and frozen soils [14]. In these cases, the original state-dependent FSD equation [9] was no longer applicable. Note that the above p', q, and e are mean effective stress, deviator stress, and void ratio, respectively. Definitions of all the stress notations follow the conventions in CSSM [15], which can be found in the Appendix.

This note aims to extend the previous FSD equation [9] by using CSLs with arbitrary form in the p'–q and e–p' planes. The note is structured as follows: Section 2 provides detailed derivations of the unified FSD equation based on arbitrary CSLs; Section 3 verifies the proposed equation by simulating a series of test results of soils with curved CSLs; Section 4 concludes the study. For the sake of simplicity, all the derivations are carried out in triaxial stress space. For more complex loading state, one can refer to Sun and Sumelka [10] or Lu *et al.* [16].

2. Unified FSD equation

In fractional plasticity, the plastic flow of soil is determined by conducting fractional derivatives of the yielding surface. Following previous studies [9,10], the Modified Cam-clay function (f) [15] is used, such that,

$$f = q^2 + M_g^2 p'^2 - M_g^2 p' p'_0 = 0, \tag{1}$$

where p'_0 is the intercept of f with the p'-axis. M_g is the gradient of the CSL in the p'–q plane, which is usually regarded as constant (e.g., M_c) for sand and clay [17]. However, for highly crushable aggregates, for example, rockfill [12] and ballast [13], M_g can be varied with pressure. For arbitrary CSL as shown in Figure 1, one can write the following general formula

$$q = g(p'), \tag{2}$$

where g is the function describing the CSL of soil in the p'–q plane. Then, $M_g = \partial g(p')/\partial p'$. Table 1 lists several different expressions of g. It can be found that the CSLs may differ from those of sand and clay. However, no matter what kind of g was used, the current stress within soil would have two relative positions before reaching the CSL. As discussed in Sun *et al.* [9], one is above the CSL (point A), the other is below the CSL (point B). For stress point A, $p' < p'_c$, $q > q_c$: the right-sided fractional derivative shown in Equation (A.2) is used for $\partial^\alpha f/\partial p'^\alpha$; whereas for the left-sided one, Equation (A.1), is used for $\partial^\alpha f/\partial q^\alpha$. Similarly, for stress point B, Equations (A.1) and (A.2) are used for $\partial^\alpha f/\partial p'^\alpha$ and $\partial^\alpha f/\partial q^\alpha$, respectively. So, the stress-dilatancy ratio (d_g) at current stress point can be defined as

$$d_g = -\frac{\partial^\alpha f/\partial p'^\alpha}{\partial^\alpha f/\partial q^\alpha}. \tag{3}$$

As the fractional derivatives are defined in integral form, the current stresses (p', q) and their target critical-state stresses (p'_c, q_c) at the CSL are defined as the lower or higher limit for integration, in previous work [9]. p'_c and q_c are connected by using the linear CSL as $q_c = q + M_c(p' - p'_c)$.

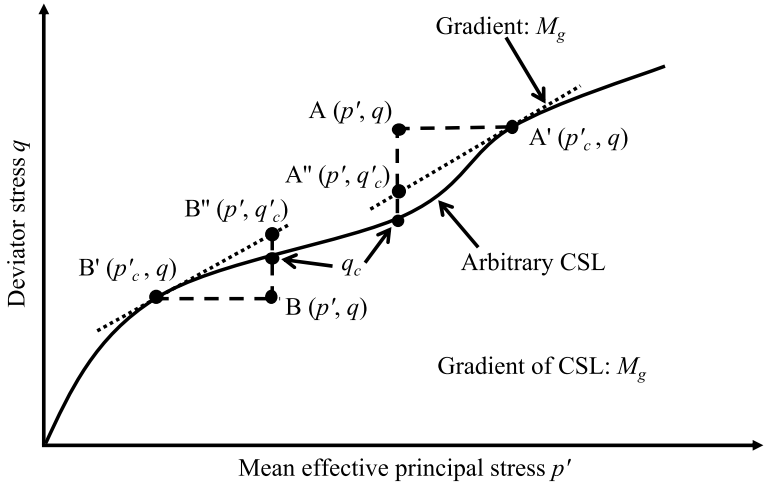

Figure 1. Schematic show of the arbitrary CSL and current stress points A/B.

However, for nonlinear CSL, the gradient between (p'_c, q) and (p', q_c) is no longer a constant (M_c). Due to the complex form of the nonlinear CSL, it would be hard to determine the value of such gradient. So, a pseudo critical-state stress, q'_c , shown in Figure 1, is defined and used instead of q_c as one of the integral limit. q'_c is the intercept of the vertical line starting from (p', q) with the tangent line passing through (p'_c, q). Accordingly, one can write

$$q'_c = q + \left.\frac{\partial g}{\partial p'}\right|_{p'=p'_c} (p' - p'_c) \tag{4}$$

$$d_g = -\frac{{}_{p'}D^{\alpha}_{p'_c} f(p')}{{}_{q'_c}D^{\alpha}_{q} f(q)} = -\frac{{}_{p'_c}D^{\alpha}_{p'} f(p')}{{}_{q}D^{\alpha}_{q'_c} f(q)}. \tag{5}$$

Substituting (4) into (5) and performing calculation, one has the following unified FSD equation for arbitrary CSL (g):

$$d_g = \left(\left.\frac{\partial g}{\partial p'}\right|_{p'=p'_c}\right)^{\alpha-1} \left(\frac{\partial g}{\partial p'}\right)^2 \frac{(p' - p'_c) + (2-\alpha)(p'_c - p'_0/2)}{(1-\alpha)(p' - p'_c)\left.\frac{\partial g}{\partial p'}\right|_{p'=p'_c} + (2-\alpha)q}. \tag{6}$$

On continuous shearing, (p', q) would gradually approach the CSL, where $q \to q'_c$ and $q'_c \to q_c$. Once reaching the critical state, the pseudo critical-state stress (q'_c) would reach the real target stress (q_c) at the CSL. In this case, $p' = p'_c$, $q = q_c$, and $d_g = 0$, which conforms to the basic regulation in CSSM. If a linear CSL is used, that is, $\partial g/\partial p' = M_c$, then (6) reduces to the original FSD equation proposed by Sun *et al.* [9].

3. Validation of the approach

To verify the unified FSD equation, a series of reported test results of ballast [13] and rockfill [18] with curved CSLs are simulated and discussed. Nonlinear expressions of the CSLs used for ballast and rockfill are shown in Table 1, while their shapes can be found in Figure 2. It can be found that due to particle degradation of ballast and rockfill, both CSLs exhibit downward bending with the increasing mean effective pressure, when compared to the linear CSL with $M_c = 2.12$. A lower extent of curve bending can be observed in rockfill. This can be partially attributed to

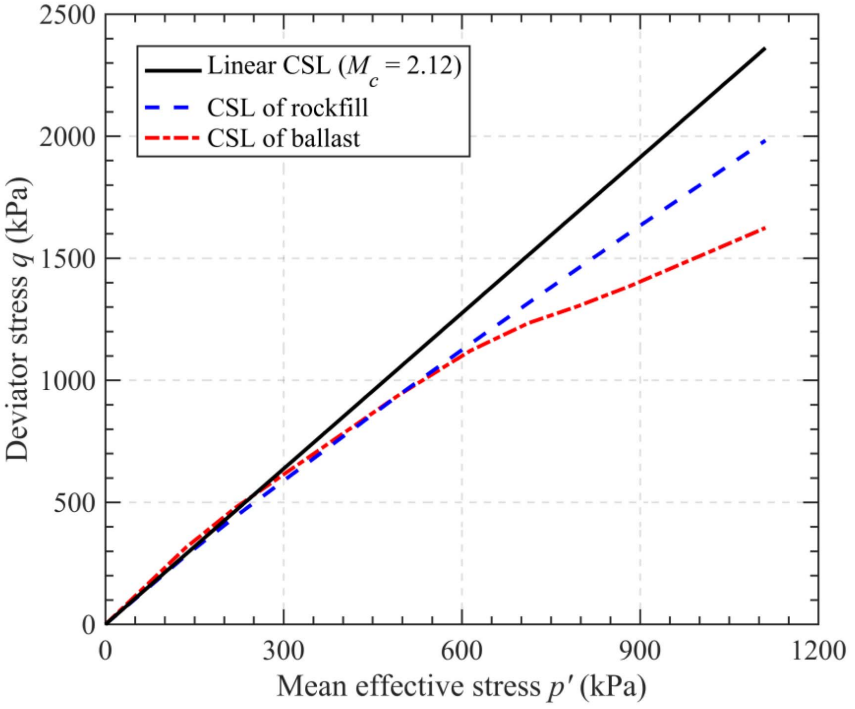

Figure 2. CSLs of ballast [13] and rockfill [18].

Table 1. Different CSLs

References	p'–q plane	e–p' plane
Ballast [13]	$g(p') = \{M_0 - [1 - \exp(-\beta BBI)]\}p'$, $BBI = \dfrac{\theta_b - \theta_b \exp(-\nu_b \varepsilon_s^{\mathrm{p}})}{\omega_b - \ln p'_{i0}}$	$e = \Gamma_{\mathrm{ref}} - a\exp(bBBI) - \lambda \ln p'$
Rockfill [18]	$g(p') = \dfrac{6\sin\varphi_{\mathrm{cs}}}{3 - \sin\varphi_{\mathrm{cs}}} p'$, $\varphi_{\mathrm{cs}} = \varphi_{\mathrm{cs0}} - \varphi_{\mathrm{csd}} \log(p'/p_a)$	$e = e_a - k_e e_0 - \lambda \left(\dfrac{p'}{p_a}\right)^{\xi}$
Sand/Clay [15]	$g(p') = M_{\mathrm{c}} p'$	$e = e_\Gamma - \lambda \ln p'$

the better initial particle size distribution of rockfill shown Figure 3, which reduced the extent of particle degradation. As discussed before, such curve bending should result in a series of tangential lines with varying gradient, $(\partial g/\partial p')|_{p'=p'_{\mathrm{c}}}$, during loading. Then, the corresponding pseudo critical-state deviator stress, q'_{c}, can be determined for further constitutive modelling of ballast and rockfill, respectively, by using (4). The relevant constitutive relations are included in the Appendix. Table 2 lists the values of each model constant used for simulation. Methods for identifying model parameters are briefly described in Table 2. For more details, one can refer to each relevant literature [9, 13, 18]. There are seven common model parameters that are shared for simulating the stress–strain behaviour of ballast and rockfill. However, depending on the specific functions to describe the shapes of the CSLs of ballast and rockfill, more parameters can be

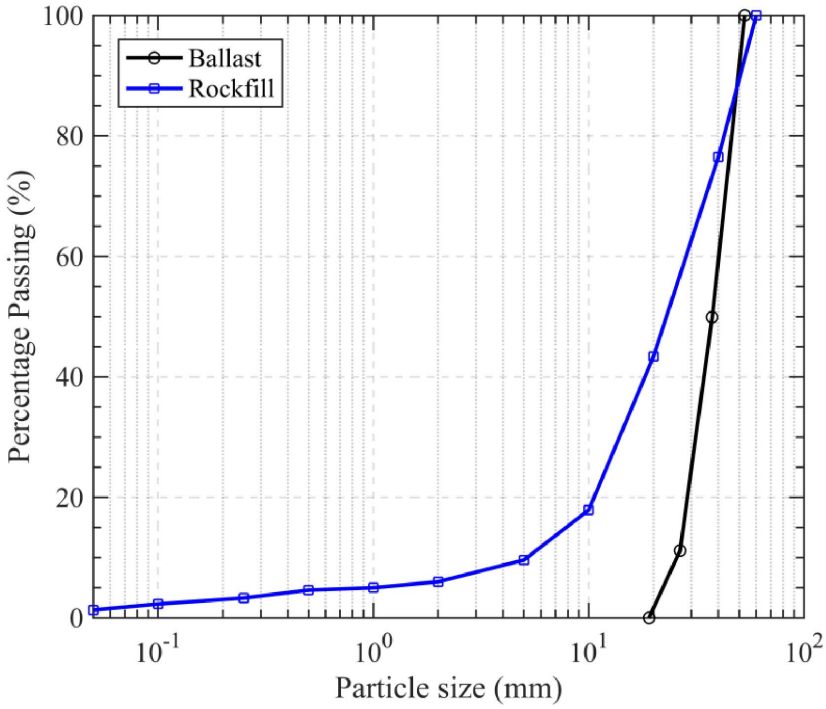

Figure 3. Particle size distributions of ballast [13] and rockfill [18].

required. For example, Indraratna *et al.* [13] introduced another eight parameters to capture the bending CSL of ballast, while Xiao *et al.* [18] proposed another five parameters for the curved CSL of rockfill, as shown in Table 2. These two sets of parameters work independently for different materials.

Figure 4 verifies the unified FSD equation by simulating the triaxial behaviour of ballast [13]. The material was reported to consist of angular/subangular particles. All the samples were prepared by layered compaction method to have an initial diameter of 300 mm and a height of 600 m. Then, monotonic triaxial tests with an axial strain rate at 0.25%/min were carried out on samples with an initial void ratio (e_0) of 0.72. It is found that the model simulations show an overall agreement with the experimental data obtained under different confining pressures (σ'_{con}). However, the model does not well capture the shear stress–strain of ballast when the consolidation stress decreases. For lower consolidation stress, a maximum of shear resistance followed by a strain softening behaviour should take place. This could be attributed to the initially large critical-state stress ratio (M_0), which results in the overestimation of the hardening potential of ballast by the hardening modulus used in this study. The relationship between volumetric strain and shear strain can be well reproduced by using the unified FSD equation. The simulated critical-state stress (p'_{c}) first increases and then decreases with the increasing shear strain. On sufficient shearing, the critical-state stress and current stress coincide, indicating the arrival of the critical state within ballast.

Figure 5 verifies the unified FSD equation by simulating the triaxial behaviour of rockfill [18]. It was reported that the rockfill material consisted of round/subround particles. The layered compaction method was used to prepare each sample with an initial height of 600 mm and a diameter of 300 mm. Then, monotonic triaxial tests with an axial strain rate at 1 mm/min were

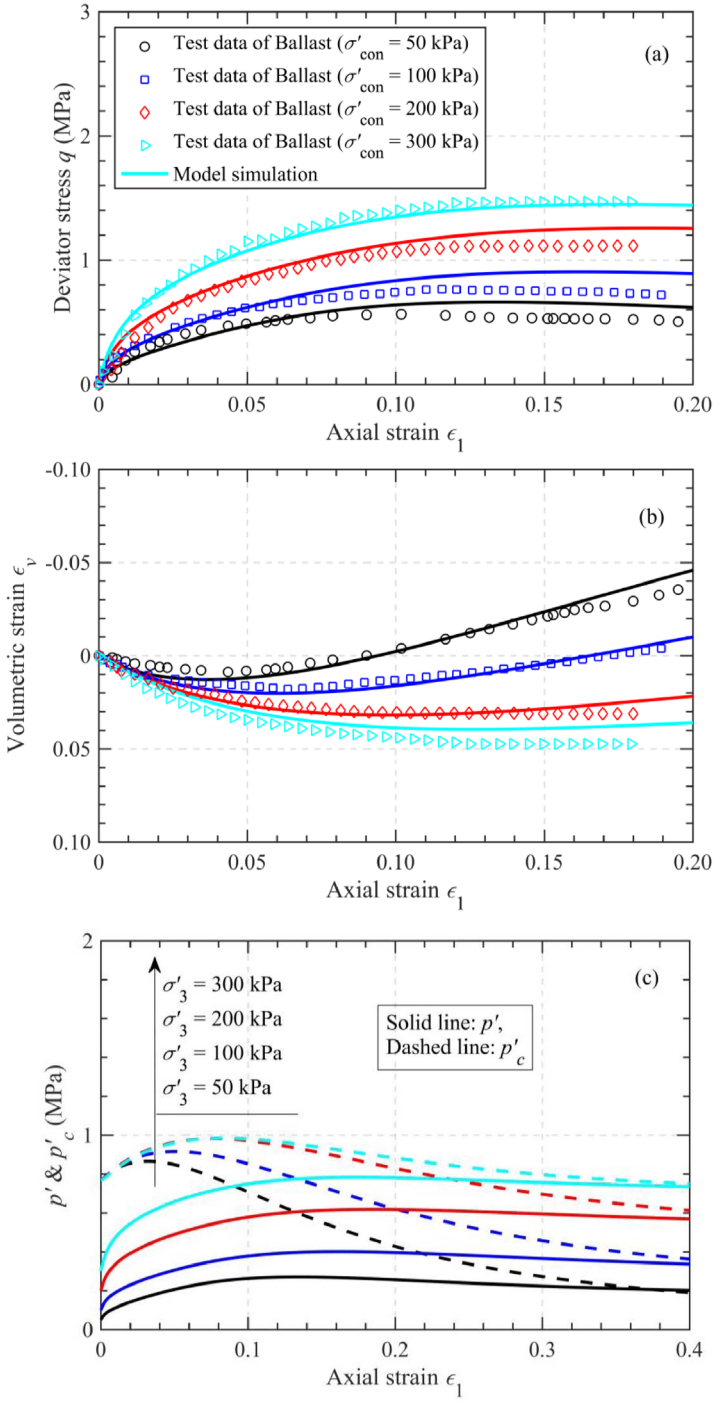

Figure 4. Validation against test data of ballast [13].

Table 2. Model parameters

Description	Parameter	Value	Methods for parameter identification
Parameters proposed in [13] for describing the CSL of ballast	Γ_{ref}	0.955	Measure the CSL intercept at p'-axis
	a	0.95	Fit the CSL data in the e–p' plane
	b	0.1	Fit the CSL data in the e–p' plane
	β	0.938	Fit the CSL data in the p'–q plane
	θ_b	0.33	Fit the BBI-ε_s^{p} relation
	υ_b	11.5	Fit the BBI-ε_s^{p} relation
	ω_b	6.4	Fit the BBI-ε_s^{p} relation
	M_0	2.10	Measure the CSL intercept at q-axis
Parameters proposed in [18] for describing the CSL of rockfill	ξ	0.7	Fit the CSL data in the p'–q plane
	φ_{cs0}	51.7	Fit the CSL data in the φ_{c}–p' plane
	$\varphi_{\text{cs}d}$	7.92	Fit the CSL data in the φ_{c}–p' plane
	e_a	0.194	Fit the CSL data in the e–p' plane
	k_e	0.55	Fit the CSL data in the e–p' plane
Parameters proposed by Sun *et al.* [9]	λ	0.155 for ballast 0.01 for rockfill	Fit the CSL data in the e–p' plane
	α	0.99 for ballast 1.05 for rockfill	Calculated from $d_g = 0$
	m	0.45 for ballast 0.30 for rockfill	Calculated from $H = 0$
	h_1	1.6 for ballast 1.2 for rockfill	Fit the q–ε_1^{p} relation
	h_2	1.6 for ballast 1.2 for rockfill	Fit the q–ε_1^{p} relation
	G_0	73 for ballast 127 for rockfill	Fit the initial q–ε_s^{p} relation
	ν	0.3 for ballast 0.25 for rockfill	Fit the initial ε_1^{p}–ε_3^{p} relation

carried out on samples with an e_0 of 0.317. It can be observed that the developed approach also simulates the triaxial behaviour of rockfill. However, when compared to the stress–strain behaviour of ballast, rockfill exhibits less stiff response at the initial loading stage. This can be attributed to the round/subround particle shape, higher aggregate crushing value (39.2%) and higher coefficient of uniformity (C_u = 5.54) of rockfill, which made the samples easier to be compacted [19]. In contrast, the angular particle shape, lower aggregate crushing value (12%), and lower coefficient of uniformity (C_u = 1.5) of ballast increased the extent of interlocking between ballast aggregates and its resistance to external loading, which thus resulted in a stiffer response of ballast under shearing [20, 21]. It can be further found in Figure 5(b) that both the volumetric response and hardening/softening can be reasonably captured. Similar to ballast, the simulated critical-state stress at low confining pressure also exhibit at first an increase and then decrease with the increasing shear strain. However, those materials sheared under higher confining pressure only exhibit monotonic increase of the critical-state pressure. However, irrespective of the initial pressure, the critical-state stress and current stress coincide upon sufficient shearing, indicating the arrival of the critical state within rockfill.

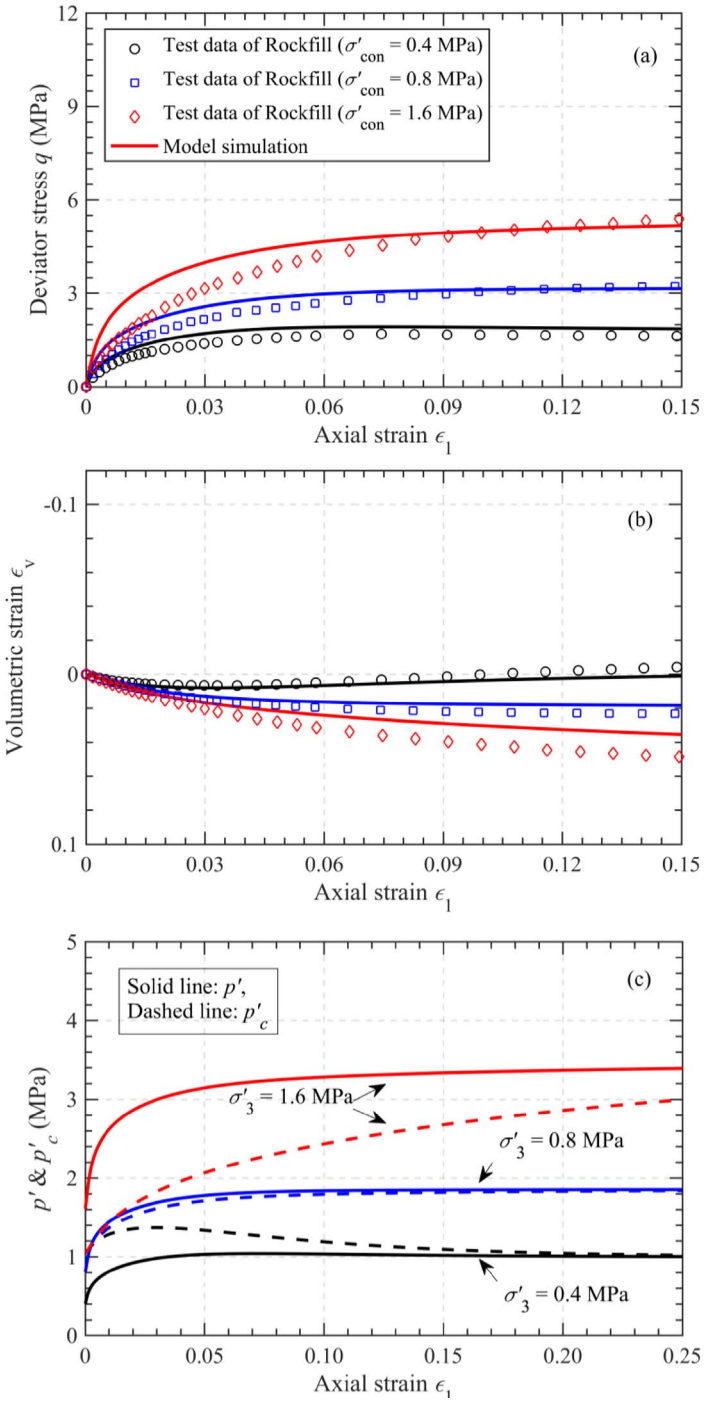

Figure 5. Validation against test data of rockfill [18].

4. Conclusions

This study made an attempt to extend the previous FSD equation for state-dependent granular materials with arbitrary CSLs. The main findings are summarised as follows:

(1) A pseudo critical-state deviator stress was proposed to act as one of the integral limits for conducting fractional derivative, where a unified FSD equation was developed.
(2) The developed FSD equation did not rely on a specific critical state response. It could be applied in soils with arbitrary type of CSL. The values of p', q, $p' - p'_{\mathrm{c}}$ together determined the evolution of the FSD equation.
(3) Further validation against a series of experimental results showed that the unified FSD equation can reasonably capture the stress–strain behaviour of different granular materials.

List of Notations

α	Fractional order
β	Critical-state parameter in [13]
ε_v	Volumetric strain
ε_s	Generalised shear strain
ε_1	Major principal strain
ε_3	Minor principal strain
φ_{cs0}	Critical-state friction angle at $p' = p_a$ [18]
$\varphi_{\mathrm{cs}d}$	Critical-state friction angle due to pressure dependence [18]
σ'	Effective normal stress component
σ'_1	Major effective principal stress
σ'_2	Medium effective principal stress
σ'_3	Minor effective principal stress
σ'_{c}	Critical-state stress
σ'_{con}	Confining pressure
η	Stress ratio
λ	Gradient of the critical state line
Γ_{ref}	Intercept of the critical state line in [13]
ξ	Critical-state parameter in [18]
ν	Poisson's ratio
ν_b	Critical-state parameter in [13]
θ_b	Critical-state parameter in [13]
ω_b	Critical-state parameter in [13]
BBI	Particle breakage ratio in [13]
d_g	Stress-dilatancy ratio
d_f	Stress ratio for defining plastic loading
D	Partial derivation
e	Current void ratio
e_0	Initial void ratio
e_a	Critical-state parameter in [18]
f	Yielding function
G	Shear modulus
G_0	Elastic constant

H Hardening modulus
h_0 Hardening function
h_1 Hardening parameter
h_2 Hardening parameter
k_e Critical-state parameter in [18]
m Peak state parameter
m_v Compression-related flow direction
m_s Shear-related flow direction
M_0 Critical-state stress ratio in [13]
M_c Constant critical-state stress ratio
M_g Variable critical-state stress ratio
M_p Drained peak stress ratio
n_v Dompression-related loading direction
n_s Shear-related loading direction
n Positive integer
p' Mean effective stress
p'_c Mean effective stress at critical state
p'_0 Intercept between the yielding surface and abscissa
q_c Deviator stress at critical state
q Deviator stress

Acknowledgements

The author would like to thank Professor Wen Chen for his lifelong inspiration. The financial support provided by the National Natural Science Foundation of China (Grant Nos. 51890912, 51679068), the Natural Science Foundation of the Jiangsu Higher Education Institutions of China (Grant No. 18KJB560006), the National Science Foundation for Post-doctoral Scientists of China (Grant No. 2019M661710) and the Alexander von Humboldt Foundation, Germany are appreciated.

Appendix

The Caputo fractional derivatives [22] are defined as:

$$ {}_{\sigma'_c}D^{\alpha}_{\sigma'} f(\sigma') = \frac{1}{\Gamma(n-\alpha)} \int_{\sigma'_c}^{\sigma'} \frac{f^{(n)}(\chi)\,\mathrm{d}\chi}{(\sigma'-\chi)^{\alpha+1-n}}, \quad \sigma' > \sigma'_c \tag{A.1} $$

$$ {}_{\sigma'}D^{\alpha}_{\sigma'_c} f(\sigma') = \frac{(-1)^n}{\Gamma(n-\alpha)} \int_{\sigma'}^{\sigma'_c} \frac{f^{(n)}(\chi)\,\mathrm{d}\chi}{(\chi-\sigma')^{\alpha+1-n}}, \quad \sigma'_c > \sigma', \tag{A.2} $$

where D means derivation. σ'_c and σ' are the critical-state stress and current stress, respectively, defining the integral limits. $\alpha \in (n-1, n)$ is the fractional order. $n = 1$ or 2. Γ is the gamma function [23].

The following stress and strain notations are used: $p' = (\sigma'_1 + 2\sigma'_3)/3$, $q = \sigma'_1 - \sigma'_3$, $\varepsilon_v = \varepsilon_1 + 2\varepsilon_3$, and $\varepsilon_s = 2(\varepsilon_1 - \varepsilon_3)/3$, where σ'_1, σ'_3, ε_1 and ε_3 are the major effective stress, minor effective stress, major strain and minor strain, respectively. If the superscripts, e and p, are imposed on the strain notation, then the elastic (ε^{e}) and plastic (ε^{p}) strain components are indicated, respectively. In addition, the critical-state stress ratio is defined as

$$ M_g = \frac{6\sin\varphi_c}{3-\sin\varphi_c}, \tag{A.3} $$

where φ_c is the critical-state friction angle. The elastoplastic relation is used in this study for model validation, such that

$$\begin{bmatrix}\Delta\varepsilon_v\\ \Delta\varepsilon_s\end{bmatrix}=\begin{bmatrix}\dfrac{1}{K}+\dfrac{m_v n_v}{H} & \dfrac{m_v n_s}{H}\\ \dfrac{m_s n_v}{H} & \dfrac{1}{3G}+\dfrac{m_s n_s}{H}\end{bmatrix}\begin{bmatrix}\Delta p'\\ \Delta q\end{bmatrix}, \tag{A.4}$$

where Δ indicates increment. K and G are the bulk and shear moduli, respectively.

$$K = (2+2\nu)G/3/(1-2\nu) \tag{A.5}$$

$$G = G_0(2.97-e)^2/(1+e)\sqrt{p' p_a}, \tag{A.6}$$

where ν and G_0 are the Poisson's ratio and elastic constant, respectively. $p_a = 100$ kPa is the atmospheric pressure. The plastic loading direction (n_v, n_s), flow direction (m_v, m_s), and hardening modulus (H) can be defined as

$$[n_v, n_s]^T = \frac{1}{\sqrt{1+d_f^2}}[d_f, 1]^T \tag{A.7}$$

$$[m_v, m_s]^T = \frac{1}{\sqrt{1+d_g^2}}[d_g, 1]^T \tag{A.8}$$

$$H = (h_1 - h_2 e)G\frac{M_p-\eta}{\eta}, \tag{A.9}$$

where h_1 and h_2 are material constants; $M_p = M_g[1 + m(\sqrt{p_c/p'} - 1)]$, in which m is material constant. $\eta = q/p'$; $d_f = d_g|_{\alpha=1}$.

References

[1] Y. P. Yao, D. A. Sun, T. Luo, "A critical state model for sands dependent on stress and density", *Int. J. Numer. Anal. Methods Geomech.* **28** (2004), p. 323-337.

[2] X. S. Shi, J. Yin, J. Zhao, "Elastic visco-plastic model for binary sand-clay mixtures with applications to one-dimensional finite strain consolidation analysis", *J. Eng. Mech.* **145** (2019), article no. 04019059.

[3] K. Been, M. G. Jefferies, "A state parameter for sands", *Géotechnique* **35** (1985), p. 99-112.

[4] K. Been, M. Jefferies, J. Hachey, "The critical state of sands", *Géotechnique* **41** (1991), p. 365-381.

[5] M. Tafili, T. Triantafyllidis, "State-dependent dilatancy of soils: experimental evidence and constitutive modeling", in *Recent Developments of Soil Mechanics and Geotechnics in Theory and Practice* (T. Triantafyllidis, ed.), Springer International Publishing, Cham, 2020, p. 54-84.

[6] D. Yin, H. Wu, C. Cheng, Y. Chen, "Fractional order constitutive model of geomaterials under the condition of triaxial test", *Int. J. Numer. Anal. Methods Geomech.* **37** (2013), p. 961-972.

[7] Y. Xiao, Z. Sun, A. M. Stuedlein, C. Wang, Z. Wu, Z. Zhang, "Bounding surface plasticity model for stress–strain and grain-crushing behaviors of rockfill materials", *Geosci. Front.* **11** (2020), p. 495-510.

[8] S. Jocković, M. Vukićević, "Bounding surface model for overconsolidated clays with new state parameter formulation of hardening rule", *Comput. Geotech.* **83** (2017), p. 16-29.

[9] Y. Sun, Y. Gao, Y. Shen, "Mathematical aspect of the state-dependent stress-dilatancy of granular soil under triaxial loading", *Géotechnique* **69** (2019), p. 158-165.

[10] Y. Sun, W. Sumelka, "State-dependent fractional plasticity model for the true triaxial behaviour of granular soil", *Arch. Mech.* **71** (2019), p. 23-47.

[11] F. Yu, "Influence of particle breakage on behavior of coral sands in triaxial tests", *Int. J. Geomech.* **19** (2019), article no. 04019131.

[12] M. Liu, Y. Zhang, H. Zhu, "3D elastoplastic model for crushable soils with explicit formulation of particle crushing", *J. Eng. Mech.* **143** (2017), article no. 04017140.

[13] B. Indraratna, Q. Sun, S. Nimbalkar, "Observed and predicted behaviour of rail ballast under monotonic loading capturing particle breakage", *Can. Geotech. J.* **52** (2014), p. 73-86.

[14] Y. Lai, M. Liao, K. Hu, "A constitutive model of frozen saline sandy soil based on energy dissipation theory", *Int. J. Plast.* **78** (2016), p. 84-113.

[15] A. Schofield, P. Wroth, *Critical State Soil Mechanics*, McGraw-Hill London, New York, USA, 1968.

[16] D. Lu, J. Liang, X. Du, C. Ma, Z. Gao, "Fractional elastoplastic constitutive model for soils based on a novel 3D fractional plastic flow rule", *Comput. Geotech.* **105** (2019), p. 277-290.
[17] V. Bandini, M. R. Coop, "The influence of particle breakage on the location of the critical state line of sands", *Soils Found.* **51** (2011), p. 591-600.
[18] Y. Xiao, H. Liu, Y. Chen, J. Jiang, W. Zhang, "State-dependent constitutive model for rockfill materials", *Int. J. Geomech.* **15** (2014), article no. 04014075.
[19] D. Sarkar, M. Goudarzy, D. König, "An interpretation of the influence of particle shape on the mechanical behavior of granular material", *Granul. Matter* **21** (2019), p. 53.
[20] Y. Sun, B. Indraratna, S. Nimbalkar, "Three-dimensional characterisation of particle size and shape for ballast", *Geotech. Lett.* **4** (2014), p. 197-202.
[21] Y. Sun, C. Zheng, "Breakage and shape analysis of ballast aggregates with different size distributions", *Particuology* **35** (2017), p. 84-92.
[22] M. Caputo, "Linear models of dissipation whose Q is almost frequency independent-II", *Geophys. J. Int.* **13** (1967), p. 529-539.
[23] H. Sun, Y. Zhang, D. Baleanu, W. Chen, Y. Chen, "A new collection of real world applications of fractional calculus in science and engineering", *Commun. Nonlinear Sci. Numer. Simul.* **64** (2018), p. 213-231.